DNA elasticity from coarse-grained simulations: The effect of groove asymmetry

Enrico Skoruppa,[1] Michiel Laleman,[1] Stefanos K. Nomidis,[1,2] and Enrico Carlon[1]
[1]*Institute for Theoretical Physics, KU Leuven, Celestijnenlaan 200D, 3001 Leuven, Belgium*
[2]*Flemish Institute for Technological Research (VITO), Boeretang 200, B-2400 Mol, Belgium*

(Received 23 March 2017; accepted 10 May 2017; published online 6 June 2017)

It is well established that many physical properties of DNA at sufficiently long length scales can be understood by means of simple polymer models. One of the most widely used elasticity models for DNA is the twistable worm-like chain (TWLC), which describes the double helix as a continuous elastic rod with bending and torsional stiffness. An extension of the TWLC, which has recently received some attention, is the model by Marko and Siggia, who introduced an additional twist-bend coupling, expected to arise from the groove asymmetry. By performing computer simulations of two available versions of oxDNA, a coarse-grained model of nucleic acids, we investigate the microscopic origin of twist-bend coupling. We show that this interaction is negligible in the oxDNA version with symmetric grooves, while it appears in the oxDNA version with asymmetric grooves. Our analysis is based on the calculation of the covariance matrix of equilibrium deformations, from which the stiffness parameters are obtained. The estimated twist-bend coupling coefficient from oxDNA simulations is $G = 30 \pm 1$ nm. The groove asymmetry induces a novel twist length scale and an associated renormalized twist stiffness $\kappa_t \approx 80$ nm, which is different from the intrinsic torsional stiffness $C \approx 110$ nm. This naturally explains the large variations on experimental estimates of the intrinsic stiffness performed in the past. *Published by AIP Publishing.* [http://dx.doi.org/10.1063/1.4984039]

I. INTRODUCTION

Owing to its role as the carrier of genetic information, DNA is of central importance in biology. In its interactions with other biomolecules within the cell, DNA is often bent and twisted. A good mechanical model of DNA is therefore essential to understand the complex biological processes in which it is involved.[1] A large number of experiments in the past have shown that its mechanical response can be described using simple continuous polymer models (studies of such models can be found, e.g., in Refs. 2–4), such as the twistable worm-like chain (TWLC), which treats DNA as an elastic rod, exhibiting resistance to applied bending and twisting.[5] In spite of its simplicity, the TWLC has proven to be surprisingly accurate in the description of the DNA response to applied forces[2,6] and torques.[7,8]

As experimental techniques become more accurate, physical models are put to increasingly strict tests. Single-molecule experiments of the past few years have reported some discrepancies between the TWLC predictions and the observed torsional response of DNA.[9,10] These experiments use magnetic tweezers in order to apply both a torque and a stretching force to a single DNA molecule. The measured torsional stiffness as a function of the applied force turned out to deviate from the TWLC predictions. A recent study explained these discrepancies using an elastic DNA model, which extends the TWLC by including a direct coupling term between the twisting and bending degrees of freedom.[11] The existence of twist-bend coupling was already predicted by Marko and Siggia[12] in 1994. Quite surprisingly the consequence of this coupling on the structural and dynamical properties of DNA has only been discussed in a very limited number of papers so far.[13,14]

In this paper, we investigate the elastic properties of oxDNA, a coarse-grained model for simulations of single- and double-stranded DNA.[15] oxDNA comes in two versions: the original version (oxDNA1) contains symmetric grooves, while in a more recent extension (oxDNA2) distinct major and minor grooves were introduced.[16] By comparing the two versions, we deduce the effect of an asymmetric grooving on the elastic properties of the molecule. Our analysis shows a clear signature of twist-bend coupling in oxDNA2, while this interaction is absent in the symmetric oxDNA1. This confirms the predictions of Marko and Siggia[12] and shows that the groove asymmetry strongly affects the elastic properties of the molecule. Our estimate of the twist-bend coupling constant in oxDNA2 is in agreement with that obtained from a recent analysis of magnetic tweezers data.[11]

II. MODELS AND SIMULATIONS

A. Elasticity models

Elastic polymer models describe double-stranded DNA as a continuous inextensible rod. At every point along the molecule, one defines a local frame of reference, given by a set of three orthonormal vectors $\{\hat{\mathbf{e}}_1(s), \hat{\mathbf{e}}_2(s), \hat{\mathbf{e}}_3(s)\}$, where $0 \le s \le L$ is the arc-length coordinate and L is the contour length. The common convention is to choose $\hat{\mathbf{e}}_3$ as the local tangent to the curve (see Fig. 1), whereas $\hat{\mathbf{e}}_1$ and $\hat{\mathbf{e}}_2$ lie in the plane of the ideal, planar Watson-Crick base pairs.[12] The vector $\hat{\mathbf{e}}_1$

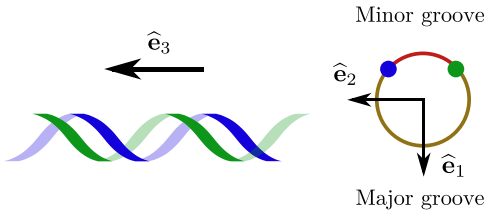

FIG. 1. DNA can be represented as an inextensible, twistable, elastic rod. Its conformation is described by a local orthonormal frame, associated with every point along the molecule. $\hat{\mathbf{e}}_3$ is the unit tangent vector, whereas $\hat{\mathbf{e}}_1$ is chosen to lie on the symmetry plane of the grooves. The third vector is given by $\hat{\mathbf{e}}_2 = \hat{\mathbf{e}}_3 \times \hat{\mathbf{e}}_1$.

is directed along the symmetry axis of the two grooves and $\hat{\mathbf{e}}_2$ is obtained from the relation $\hat{\mathbf{e}}_2 = \hat{\mathbf{e}}_3 \times \hat{\mathbf{e}}_1$. Knowing how the set $\{\hat{\mathbf{e}}_1(s), \hat{\mathbf{e}}_2(s), \hat{\mathbf{e}}_3(s)\}$ depends on s allows one to reconstruct the conformation of the molecule.

Any local deformation of the curve induces a rotation of the frame $\{\hat{\mathbf{e}}_1, \hat{\mathbf{e}}_2, \hat{\mathbf{e}}_3\}$ from s to $s + ds$, which can be described by the following differential equation:

$$\frac{\mathrm{d}\hat{\mathbf{e}}_\mu}{\mathrm{d}s} = (\boldsymbol{\Omega} + \omega_0 \hat{\mathbf{e}}_3) \times \hat{\mathbf{e}}_\mu, \tag{1}$$

where $\mu = 1, 2, 3$ and ω_0 is the intrinsic twist density of the DNA double helix. The vector $\boldsymbol{\Omega} + \omega_0 \hat{\mathbf{e}}_3$ is parallel to the axis of rotation from $\hat{\mathbf{e}}_\mu(s)$ to $\hat{\mathbf{e}}_\mu(s + ds)$. Note that in general $\boldsymbol{\Omega}(s)$ depends on the coordinate s. Decomposing this vector along the local frame, we define its three components as $\Omega_\mu(s) \equiv \boldsymbol{\Omega} \cdot \hat{\mathbf{e}}_\mu(s)$. The case $\boldsymbol{\Omega} = |\boldsymbol{\Omega}|\hat{\mathbf{e}}_3$ corresponds to a pure twist deformation, whereas $\boldsymbol{\Omega} = |\boldsymbol{\Omega}|\hat{\mathbf{e}}_1$ and $\boldsymbol{\Omega} = |\boldsymbol{\Omega}|\hat{\mathbf{e}}_2$ express bending in the planes defined by $\hat{\mathbf{e}}_1$ and $\hat{\mathbf{e}}_2$, respectively.

The lowest-energy configuration of the system is that of zero mechanical stress $\Omega_1 = \Omega_2 = \Omega_3 = 0$, which corresponds to a straight rod with an intrinsic twist angle per unit length equal to ω_0. Expanding around this ground state, one obtains the elastic energy to the lowest order in the deformation parameters Ω_μ as

$$\beta E = \frac{1}{2} \int_0^L \sum_{\mu,\nu=1}^{3} \Omega_\mu(s) M_{\mu\nu} \Omega_\nu(s) ds, \tag{2}$$

where $\beta \equiv 1/k_\mathrm{B}T$ is the inverse temperature. The 3×3 symmetric matrix $M_{\mu\nu}$, which we refer to as the stiffness matrix, contains the elastic constants. Note that from Eq. (1) the Ω's have the dimension of inverse length. As the left-hand side of Eq. (2) is dimensionless, the elements of the stiffness matrix have the dimension of length. In this work, sequence-dependent effects will be neglected; therefore $\mathbf{M}$ will not depend on s.

Marko and Siggia[12] argued that, due to the asymmetry introduced by the major and minor grooves, the elastic energy of DNA should be invariant only under the transformation $\Omega_1 \to -\Omega_1$. This implies that $\Omega_2\Omega_3$ is the only cross term allowed by symmetry; therefore the stiffness matrix in the Marko-Siggia (MS) model becomes

$$\mathbf{M}_\mathrm{MS} = \begin{pmatrix} A_1 & 0 & 0 \\ 0 & A_2 & G \\ 0 & G & C \end{pmatrix}, \tag{3}$$

where $A_1 \equiv M_{11}$, $A_2 \equiv M_{22}$, $C \equiv M_{33}$, and $G \equiv M_{23} = M_{32}$. A_1 and A_2 express the energetic cost of a bending deformation about the local axes $\hat{\mathbf{e}}_1$ and $\hat{\mathbf{e}}_2$, respectively.[17] C is the intrinsic torsional stiffness, whereas G quantifies the twist-bend coupling interaction. Note that $G \neq 0$ is a direct consequence of the groove asymmetry in the DNA double helix. If one neglects this asymmetry, the MS model reduces to the TWLC model ($G = 0$), and the corresponding stiffness matrix becomes diagonal[12]

$$\mathbf{M}_\mathrm{TWLC} = \begin{pmatrix} A_1 & 0 & 0 \\ 0 & A_2 & 0 \\ 0 & 0 & C \end{pmatrix}. \tag{4}$$

Most studies[5] model DNA as an isotropic TWLC, for which $A_1 = A_2$.

B. Computer simulations with oxDNA

In this paper we investigate the elastic properties of oxDNA, which is a model for coarse-grained computer simulations of both single- and double-stranded DNAs.[15] The model describes double-stranded DNA as two intertwined strings of rigid nucleotides, with pairwise interactions modeling the backbone covalent bonds, the hydrogen bonding, the stacking, cross-stacking, and excluded-volume interactions. oxDNA has been used in the past for the study of a variety of DNA properties.[15,16,18,19]

We performed simulations using two available versions of the model. The first version (oxDNA1) describes DNA as a molecule with no distinction between major and minor grooves,[18] while the second (oxDNA2) introduces a distinct grooving asymmetry.[16] Figure 2 illustrates molecular conformations of the two models, including a cross sectional view of a single base pair. As discussed above, the presence of distinct major and minor grooves breaks a molecular symmetry, so we expect that oxDNA1 and oxDNA2 will be mapped onto the TWLC [Eq. (4)] and the MS model [Eq. (3)], respectively.

To sample equilibrium fluctuations, molecular dynamics simulations in the NVE ensemble with an Andersen-like thermostat were used. This is implemented in repeated cycles in which the system is first evolved by integrating Newton's equations of motion in time for a given number of steps. Then the momenta of some randomly selected particles are chosen from a Maxwell distribution with a desired simulation temperature (T = 295 K in our case). The cycle then repeats itself for a large number of times.

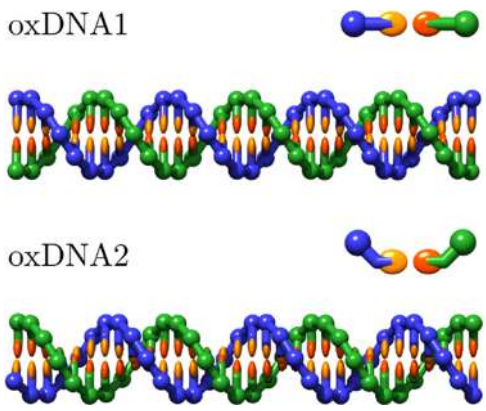

FIG. 2. Snapshots of configurations of oxDNA1 (top) and oxDNA2 (bottom), including a cross sectional view of the helix. While the grooves are symmetric in oxDNA1, distinct major and minor grooves are present in oxDNA2.

Molecular dynamics simulations were performed on 150 base pair molecules using averaged base pair interaction coefficients. A total of 5×10^{10} time steps were sampled using a numerical integration time step of 15.2 fs, and the trajectories were recorded every 5×10^4 time steps. For all simulations, the salt concentration was set to 0.5M. In oxDNA1 this value is fixed, since the electrostatic interactions are implemented through excluded-volume potentials, parametrized to mimic high salt concentration (i.e., 0.5M). oxDNA2 improved upon this approach by switching to a Debye-Hückel potential, which models the ionic screening of electrostatic interactions. This allows for the explicit selection of a salt concentration, which we set to 0.5M, in order to achieve optimal comparability between the two models.

C. Extraction of elastic parameters

The pivotal objective of the extraction of elastic parameters is to map oxDNA onto the described elastic model in such a way that both the elastic properties at the base pair level as well as long range behavior, such as bending and torsional persistence lengths, are captured as accurately as possible. Establishing an appropriate one-to-one correspondence requires the reduction of both models to the same level of complexity. For the continuous elastic model, this implies the discretization of the elastic free energy functional Eq. (2) to the base pair level

$$\beta E = \frac{a}{2} \sum_{n=1}^{N} \left(\sum_{\mu,\nu=1}^{3} \Omega_\mu^{(n)} M_{\mu\nu} \Omega_\nu^{(n)} \right), \tag{5}$$

where $a = 0.34$ nm is the mean distance between successive base pairs and $\Omega_\mu^{(n)} \equiv \Omega_\mu(na)$. In the discrete case, the finite rotation of a local frame of reference (triad) $\{\widehat{\mathbf{e}}_1(n), \widehat{\mathbf{e}}_2(n), \widehat{\mathbf{e}}_3(n)\}$, associated with the spatial orientation of the nth base pair of the molecule, into the sequentially adjacent triad $\{\widehat{\mathbf{e}}_1(n+1), \widehat{\mathbf{e}}_2(n+1), \widehat{\mathbf{e}}_3(n+1)\}$, can be represented by a rotation vector $\mathbf{\Theta}^{(n)}$. The deformation parameters $\Omega_\mu^{(n)}$ can then be defined as the deviations of the components of $\mathbf{\Theta}^{(n)}/a$ from their respective mean values,

$$a\Omega_\mu^{(n)} \equiv \Theta_\mu^{(n)} - \left\langle \Theta_\mu^{(n)} \right\rangle. \tag{6}$$

For oxDNA1 the mean twist angle $a\omega_0 = \langle \Theta_3^{(n)} \rangle$ is found to be 34.8°, whereas for oxDNA2 we find 34.1°.

Accordingly, an appropriate triad has to be assigned to each base pair of the oxDNA model. The particular choice of those triads contains a certain degree of ambiguity, resulting in different mappings for different triads. Such ambiguity regarding the definition of the tangent vector $\widehat{\mathbf{e}}_3$ in coarse-grained simulations of DNA and the related implications for the extraction of the bending persistence length has, for instance, been discussed by Fathizadeh *et al.*,[20] who showed that, when considering short length scales, different definitions of the local tangent vector will usually yield significantly different results for the bending persistence length. However, when considering longer length scales, i.e., comparing more distant tangent vectors, those discrepancies vanish asymptotically.

For a detailed discussion of different triad definitions, we refer to the supplementary material. All results presented in the main text are calculated with a triad definition employing local tangents $\widehat{\mathbf{e}}_3$ obtained from the mean vector of the intrinsic orientation of the two nucleotides in each base pair, provided by the oxDNA output. The unit vector $\widehat{\mathbf{e}}_2$ is obtained from the projection of the connecting vector between the centers of the two nucleotides $\mathbf{y}$ onto the orthogonal space of $\widehat{\mathbf{e}}_3$. Having identified $\widehat{\mathbf{e}}_3$ and $\widehat{\mathbf{e}}_2$, the remaining vector in the right-handed triad is now uniquely defined as $\widehat{\mathbf{e}}_1 = \widehat{\mathbf{e}}_2 \times \widehat{\mathbf{e}}_3$. This corresponds to Triad II in the supplementary material.

In order to infer the stiffness matrix from simulations, we used the standard procedure (see, e.g., Ref. 13) which relies on the equipartition theorem[21]

$$\left\langle \Omega_\mu^{(n)} \frac{\partial \beta E}{\partial \Omega_\nu^{(n)}} \right\rangle = \delta_{\mu\nu}, \tag{7}$$

where $\langle \cdot \rangle$ indicates the thermal average. Then we introduced the 3×3 covariance matrix with elements

$$\Lambda_{\mu\nu} \equiv \left\langle \Omega_\mu^{(n)} \Omega_\nu^{(n)} \right\rangle, \tag{8}$$

where the index n was dropped from Λ, as we neglect sequence-dependent effects. Combining (5) and (7) we get

$$\mathbf{M} = \frac{1}{a} \mathbf{\Lambda}^{-1}. \tag{9}$$

Thus, the stiffness parameters contained in $\mathbf{M}$ can be extracted from the correlation matrix $\mathbf{\Lambda}$, obtained from equilibrium fluctuations [Eq. (8)].

This procedure is based on the elastic energy being given by Eq. (5), which in turn assumes that there are no correlations between different sets of Ω's. To investigate the effect of correlations, we introduce the matrix

$$\Xi_{\mu\nu}(m) \equiv \left\langle \left[\sum_{k=n}^{n+m-1} \Omega_\mu^{(k)} \right] \left[\sum_{l=n}^{n+m-1} \Omega_\nu^{(l)} \right] \right\rangle. \tag{10}$$

If correlations beyond neighboring bases are weak, the cross terms in the previous expression can be neglected and we obtain

$$\Xi_{\mu\nu}(m) \approx \sum_{k=n}^{n+m-1} \left\langle \Omega_\mu^{(k)} \Omega_\nu^{(k)} \right\rangle = m\Lambda_{\mu\nu}. \tag{11}$$

Finally we define the $m$step stiffness matrix as

$$\mathbf{M}(m) \equiv \frac{m}{a} [\mathbf{\Xi}(m)]^{-1}, \tag{12}$$

from which the $m$step elastic constants can be obtained. In absence of correlations, this matrix will not depend on m.

III. RESULTS

We present here the results of the simulations highlighting the differences in elastic properties between oxDNA1 and oxDNA2.

A. Probability distributions

Qualitative evidence of the presence of a non-zero twist-bend coupling in the energy functionals can already be inferred from the distribution of the off-diagonal terms $\Omega_\mu^{(n)} \Omega_\nu^{(n)}$ with $\mu \neq \nu$. Figure 3 shows histograms of these quantities, obtained from simulations of oxDNA1 and oxDNA2. The data are averaged over all base pairs along the DNA contour; hence we drop

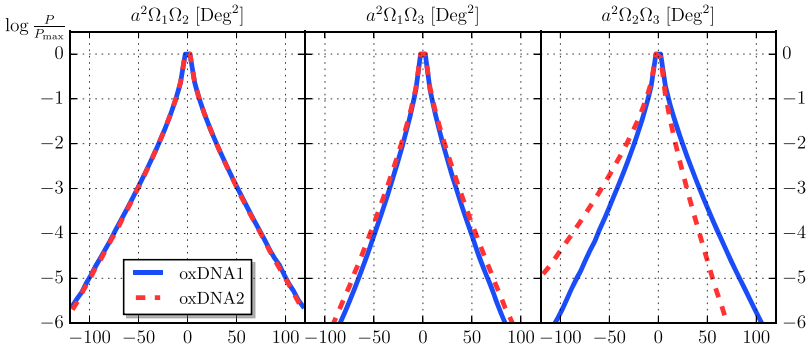

FIG. 3. Histograms of cross-diagonal terms $\Omega_\mu\Omega_\nu$ for oxDNA1 and oxDNA2. The histograms for $\Omega_1\Omega_2$ and $\Omega_1\Omega_3$ are quite similar for the two models, while there is a marked difference for $\Omega_2\Omega_3$. The asymmetric shape of the histogram in oxDNA2 is a signature of the presence of twist-bend coupling.

the position index n. While the distribution of $\Omega_1\Omega_2$ and $\Omega_1\Omega_3$ is symmetric and very similar in oxDNA1 and oxDNA2, there is a marked difference between the two models in the histogram of $\Omega_2\Omega_3$. In oxDNA1 the distribution appears to be symmetric, whereas in oxDNA2 there is a clear asymmetry, suggesting the existence of a coupling between those deformation parameters.

B. Stiffness matrix

In order to quantify the observed twist-bend coupling interaction, we computed the $m$step stiffness matrix $\mathbf{M}(m)$, as defined in Eq. (12), for both models and for different summation lengths m. At both chain-ends, 5 base pairs were excluded from this calculation, since those boundary segments are found to exhibit a significantly higher flexibility than segments located in the center of the chain. The results are shown in Fig. 4, where the elements of $\mathbf{M}(m)$ are plotted as a function of m. In both models the diagonal elements A_1, A_2, and C, as defined in Eqs. (3) and (4), have distinct, non-vanishing values. There is, however, a remarkable difference between oxDNA1 and oxDNA2 in the values of the off-diagonal elements G, M_{12}, and M_{13}. In particular, all off-diagonal elements in oxDNA1 are orders of magnitude smaller than the diagonal ones. On the other hand, although M_{12} and M_{13} remain negligibly small, the twist-bend coupling G in oxDNA2 becomes comparable in magnitude to the diagonal terms, which clearly has to be attributed to the asymmetry of the helical grooves. These results are in line with the predictions of Marko and Siggia[12] and remain valid regardless of the exact choice of coordinate systems (see the supplementary material).

As discussed in Sec. III A, in the absence of correlations between different sets of Ω's, the elements of $\mathbf{M}(m)$ are expected to be independent of m. The results of Fig. 4, however, show that this is not exactly true, which is a signature of the influence of correlations between base pairs separated by more than one nucleotide (though the convergence to a limiting value for increasing m is quite rapid).

When comparing the results among different choices of frames, we find that, despite the different values for $m = 1$, at large m all values are close to each other (see the supplementary material). We, thus, consider these limiting values to be good estimates for the stiffness parameters of the elastic model, onto which oxDNA is mapped. Table I summarizes the estimated values of the elastic parameters, averaged over the different choices of local frames, where the error bars reflect the uncertainty from estimates obtained from four different definitions of frames. The first two rows in Table I are data obtained from oxDNA simulations in this work, while the last row shows the parametrization obtained from fits of the MS model to magnetic tweezers data.[11] oxDNA2 data for C and G are consistent with the latter, while some differences are found in A_1 and A_2. It should be noted, however, that the fitting

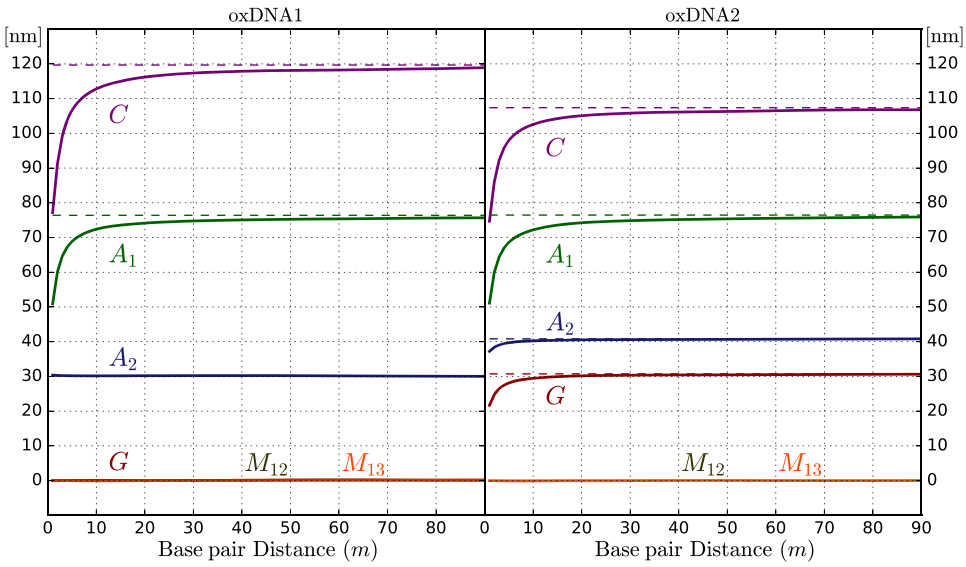

FIG. 4. Elastic parameters, obtained from the $m$step stiffness matrix, as a function of the base pair distance m. The remarkable difference between these two sets is the appearance of a significant twist-bend coupling term G for oxDNA2, in contrast to its negligible value in oxDNA1. This is in agreement with the original prediction of Marko and Siggia.[12]

TABLE I. Values of the stiffness coefficients for oxDNA1 and oxDNA2 obtained in this work (expressed in nm). The last line shows the values obtained from fitting the MS model to magnetic tweezers data.

	A_1	A_2	C	G
oxDNA1	84(14)	29(2)	118(1)	0.1(0.2)
oxDNA2	81(10)	39(2)	105(1)	30(1)
Nomidis *et al.*[11]	66	46	110(5)	40(10)

procedure used in Ref. 11 was not very sensitive to the specific choice of A_1 and A_2, as other choices fitted the experimental data equally well. The overall quantitative agreement between the oxDNA2 parameters and those from this recent study supports the choice of the plateau values in Fig. 4 as an estimate for the elastic parameters.

The value obtained for C is in good agreement with previous estimates for oxDNA, which were obtained from methods not involving the calculation of the stiffness matrix. From two independent measurements,[22,23] the value $C = 115$ nm was reported for oxDNA1. In oxDNA2 a fit of torsional stiffness data[16] gives $C = 93$–98 nm, which is slightly lower than our current estimate.

C. Persistence lengths

Any twistable polymer model is characterized by two distinct persistence lengths, related to bending and twisting fluctuations. The bending persistence length can be obtained from the decay of the correlation between tangent vectors

$$\langle \hat{\mathbf{e}}_3(n) \cdot \hat{\mathbf{e}}_3(n+m) \rangle \equiv \langle \cos\theta(m) \rangle \sim e^{-ma/l_\mathrm{b}}, \tag{13}$$

where $\theta(m)$ is the angle formed by the two vectors. As the exponential decay is valid asymptotically in m, we can estimate the bending persistence length from the extrapolation at large m of the quantity

$$l_\mathrm{b}(m) \equiv -\frac{ma}{\log\langle \cos\theta(m) \rangle}. \tag{14}$$

Analogously, we can define the twisting persistence length from the decay of the average twist angle,

$$l_\mathrm{t}(m) \equiv -\frac{ma}{\log\left\langle \cos\sum_{k=n}^{n+m-1}\Omega_3^{(k)} \right\rangle}. \tag{15}$$

Equations (14) and (15) can be compared to some analytical expressions. In the TWLC, the bending persistence length l_b is the harmonic mean of the two bending stiffnesses,[24,25]

$$l_\mathrm{b} = \frac{2A_1A_2}{A_1 + A_2}, \tag{16}$$

while the twist persistence length is just twice the torsional stiffness (see, e.g., Ref. 26),

$$l_\mathrm{t} = 2C. \tag{17}$$

The same quantities have been calculated for the MS model,[11]

$$l_\mathrm{b} = 2A_1\frac{A_2 - G^2/C}{A_1 + A_2 - G^2/C} \tag{18}$$

and

$$l_\mathrm{t} = 2C\left(1 - \frac{G^2}{A_2 C}\right). \tag{19}$$

From the last two expressions, one recovers the TWLC limit upon setting $G = 0$.

Figure 5 shows a comparison of the persistence lengths, as obtained from Eqs. (14) and (15), with the analytical expressions of the TWLC [Eqs. (16) and (17)] and the MS model [Eqs. (18) and (19)]. There is a good overall agreement between the direct computation of the persistence lengths and Eqs. (18) and (19) (with the plateau values of Fig. 4), for both oxDNA1 and oxDNA2. In particular, the prediction of the twisting persistence length is excellent in both models, whereas some small deviations are observed for l_b (smaller than 10%). This suggests that there are some features of oxDNA which are not fully captured by the "projection" to an inextensible elastic model, as described by Eq. (2). Note that l_b in oxDNA2 exhibits a damped oscillatory behavior at short lengths m with the helix periodicity, suggesting that the tangent vectors are systematically misaligned. The value of the bending persistence length calculated here is in agreement with previous published oxDNA1 and oxDNA2 data.[16,22,23]

IV. DISCUSSION

Owing to its chirality, DNA has been found to possess some remarkable mechanical properties, such as twist-bend[12] and twist-stretch coupling.[27] Although the latter has been investigated in several studies,[28–32] the effect of twist-bend coupling remains to date largely unexplored. Motivated by some recently resurgent interest,[11] we have investigated the origin of this interaction in oxDNA, a coarse-grained model of nucleic acids. Twist-bend coupling is a cross-interaction

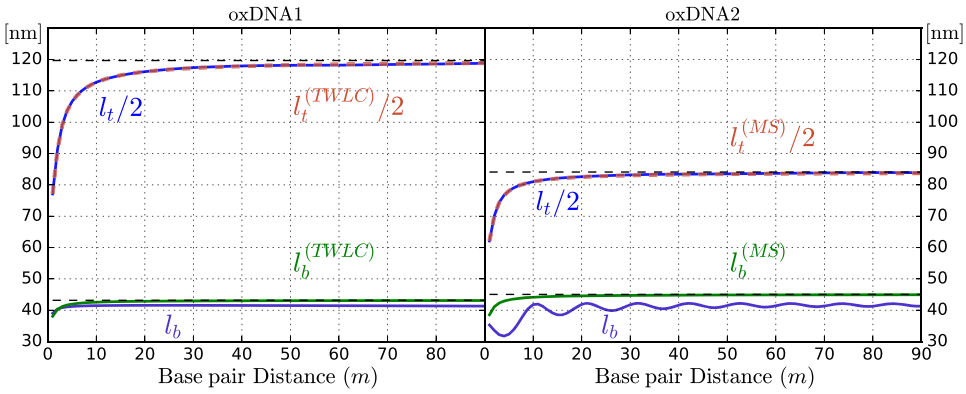

FIG. 5. Blue lines: plots of l_b and $l_\mathrm{t}/2$ obtained from oxDNA simulations using Eqs. (14) and (15). Orange and green lines: analytical predictions for the same quantities in the TWLC [Eqs. (16) and (17)] and in the MS model [Eqs. (18) and (19)], where the m-dependent stiffnesses of Fig. 4 were used. The values obtained from the plateau values of the elastic parameters are indicated by the dashed black lines.

TABLE II. Elements of the stiffness matrix (expressed in nm) for different base pairs, obtained from all-atom simulations (courtesy of Lankaš and Geršata). In order to facilitate the readout, we have included the tilt, roll, and twist nomenclature, which corresponds to our definition of Ω_1, Ω_2, and Ω_3, respectively.

	CG	CA	TA	AG	GG	AA	GA	AT	AC	GC	Average
A_1 (tilt-tilt)	47.6	50.6	44.5	67.3	70.7	60.9	69.9	73.6	75.0	70.0	63.0
A_2 (roll-roll)	27.7	31.4	24.5	41.0	44.4	42.2	38.7	45.1	46.1	47.3	38.8
C (twist-twist)	32.7	34.0	57.6	57.9	58.9	49.5	46.6	77.7	65.1	51.7	53.2
G (roll-twist)	3.7	5.8	14.1	6.7	7.4	10.5	15.7	11.9	13.4	13.0	10.2
M_{12} (tilt-roll)	2.8	1.3	0.1	−5.3	−1.7	3.6	−0.2	0.4	4.0	−0.5	0.4
M_{13} (tilt-twist)	4.4	−1.5	−1.1	−3.9	0.9	6.7	0.0	−0.7	−0.6	−0.7	0.4

between twist and bending degrees of freedom. In the context of DNA, the existence of such an interaction was predicted by Marko and Siggia,[12] who argued that twist-bend coupling follows from the groove asymmetry, a characteristic of the DNA molecular structure.

oxDNA is particularly suited to investigate the origin of twist-bend coupling, as it comes in two different versions (oxDNA1 and oxDNA2). The double helical grooves are symmetric in oxDNA1 and asymmetric in oxDNA2, with widths reproducing the average B-DNA geometry. Our simulations, sampling equilibrium conformations of both oxDNA1 and oxDNA2, show that only the latter model has a significant twist-bend coupling term (Fig. 4). This is in agreement with the symmetry argument by Marko and Siggia.[12]

The estimated twist-bend coupling coefficient from oxDNA2 is $G = 30 \pm 1$ nm, which agrees with the value $G = 40 \pm 10$ nm, obtained from fitting magnetic tweezers data.[11] An earlier estimate of $G \approx 25$ nm was obtained from the analysis of structural correlations of DNA wrapped around histone proteins.[14] It is worth noting that all-atom simulations also support the existence of a twist-bend coupling term,[13,24,33] although those studies are restricted to short fragments (≈20 bp). Table II contains the elements of one-step stiffness matrices, obtained by Lankaš *et al.*[24] from all-atom simulations.

Although the original analysis included various stretching deformations, here we only show the rotational coordinates, while the translational degrees of freedom are integrated out. The data in Table II refer to deformations between neighboring base pairs; hence they are the counterparts of the $m = 1$ data of Fig. 4 and cannot be used as reliable estimates of asymptotic values of the elastic parameters. Nonetheless, the averages over all possible sequence combinations (last column of Table II) show that twist-bend coupling is much larger than the other off-diagonal terms, i.e., $G \gg M_{12}, M_{13}$.

One of the most remarkable effects of twist-bend coupling in DNA is the appearance of a novel twist length scale[11] [Eq. (19)] with an associated twist stiffness $\kappa_t = l_t/2$, which differs from the intrinsic value C. We refer to κ_t as the renormalized twist stiffness. In the MS and TWLC models, a pure twist deformation ($\Omega_1 = \Omega_2 = 0, \Omega_3 \neq 0$) has an associated intrinsic stiffness C. In the presence of bending fluctuations ($\langle\Omega_1^2\rangle, \langle\Omega_2^2\rangle > 0$), however, the two models behave differently. While the torsional stiffness of the TWLC remains the same, in the MS model, twist deformations are governed by a lower stiffness $\kappa_t < C$. In other words, twist-bend coupling allows for the relief of twist strain by means of induced bending, therefore, making the DNA molecule torsionally softer. In other words, in the presence of bending fluctuations, twist-bend coupling makes the DNA molecule torsionally softer. From oxDNA2 simulations, we estimate $\kappa_t = l_t/2 \approx 83$ nm (see Fig. 5). This is close to the value $\kappa_t = 75$ nm, recently obtained from fitting the MS model to magnetic tweezers data.[11] The above effect naturally explains[11] some reported discrepancies in the experimental determination of C.

Having shown that the twist-bend coupling is a relevant interaction in DNA, one can ask in which limits and for which quantities the TWLC can still be considered a good DNA model. Our work shows that one can map freely fluctuating DNA onto a TWLC using $C \approx 80$ nm as the twist elastic parameter, which incorporates the effect of twist-bend coupling. However some care needs to be taken in the presence of a stretching force, as the suppression of bending fluctuation will influence the twist stiffness. At high forces, DNA will then be mapped onto an effective TWLC with a higher value of C. Finally, it will be important to investigate the effect of twist-bend coupling in cases where the DNA behavior is influenced by its mechanics as in DNA supercoiling[34,35] or in DNA-protein interactions.[36,37]

SUPPLEMENTARY MATERIAL

See supplementary material for the different triads which are defined and the corresponding stiffness parameters which are presented. Furthermore we elaborate on how to obtain the rotation vector $\boldsymbol{\Omega}$ from subsequent triads. Moreover, we explored sequence-dependent effects, by investigating some specific sequences with oxDNA. Finally, we extended the analysis of the main text to oxRNA.

ACKNOWLEDGMENTS

Discussions with F. Kriegel, F. Lankaš, J. Lipfert, C. Matek, and W. Vanderlinden are gratefully acknowledged. We thank T. Geršata for analyzing the all-atom simulation trajectories,[24] from which stiffness data in Table II were obtained. We acknowledge financial support from KU Leuven Grant No. IDO/12/08 and Research Funds Flanders (FWO Vlaanderen) Grant No. VITO-FWO 11.59.71.7N.

[1] Z. Bryant, F. C. Oberstrass, and A. Basu, "Recent developments in single-molecule DNA mechanics," Curr. Opin. Struct. Biol. **22**, 304–312 (2012).
[2] J. F. Marko and E. D. Siggia, "Stretching DNA," Macromolecules **28**, 8759–8770 (1995).
[3] J. D. Moroz and P. Nelson, "Entropic elasticity of twist-storing polymers," Macromolecules **31**, 6333–6347 (1998).

[4]J. Ubbink and T. Odijk, "Electrostatic-undulatory theory of plectonemically supercoiled DNA," Biophys. J. **76**, 2502–2519 (1999).
[5]P. Nelson, M. Radosavljevic, and S. Bromberg, *Biological Physics: Energy, Information, Life* (W. H. Freeman and Company, New York, 2002).
[6]C. Bustamante, Z. Bryant, and S. B. Smith, "Ten years of tension: Single-molecule DNA mechanics," Nature **421**, 423–427 (2003).
[7]J. F. Marko and E. D. Siggia, "Fluctuations and supercoiling of DNA," Science **265**, 506–508 (1994).
[8]T. Strick, J.-F. Allemand, D. Bensimon, A. Bensimon, and V. Croquette, "The elasticity of a single supercoiled DNA molecule," Science **271**, 1835–1837 (1996).
[9]J. Lipfert, J. W. Kerssemakers, T. Jager, and N. H. Dekker, "Magnetic torque tweezers: Measuring torsional stiffness in DNA and RecA-DNA filaments," Nat. Methods **7**, 977–980 (2010).
[10]J. Lipfert, M. Wiggin, J. W. Kerssemakers, F. Pedaci, and N. H. Dekker, "Freely orbiting magnetic tweezers to directly monitor changes in the twist of nucleic acids," Nat. Commun. **2**, 439 (2011).
[11]S. K. Nomidis, F. Kriegel, W. Vanderlinden, J. Lipfert, and E. Carlon, "Twist-bend coupling and the torsional response of double-stranded DNA" Phys. Rev. Lett. **118**, 217801 (2017).
[12]J. Marko and E. Siggia, "Bending and twisting elasticity of DNA," Macromolecules **27**, 981–988 (1994).
[13]F. Lankaš, J. Šponer, P. Hobza, and J. Langowski, "Sequence-dependent elastic properties of DNA," J. Mol. Biol. **299**, 695–709 (2000).
[14]F. Mohammad-Rafiee and R. Golestanian, "Elastic correlations in nucleosomal DNA structure," Phys. Rev. Lett. **94**, 238102 (2005).
[15]T. E. Ouldridge, A. A. Louis, and J. P. Doye, "DNA nanotweezers studied with a coarse-grained model of DNA," Phys. Rev. Lett. **104**, 178101 (2010).
[16]B. E. Snodin, F. Randisi, M. Mosayebi, P. Šulc, J. S. Schreck, F. Romano, T. E. Ouldridge, R. Tsukanov, E. Nir, and A. A. Louis, "Introducing improved structural properties and salt dependence into a coarse-grained model of DNA," J. Chem. Phys. **142**, 234901 (2015).
[17]H. Salari, B. Eslami-Mossallam, S. Naderi, and M. Ejtehadi, "Extreme bendability of DNA double helix due to bending asymmetry," J. Chem. Phys. **143**, 104904 (2015).
[18]P. Šulc, F. Romano, T. E. Ouldridge, L. Rovigatti, J. P. K. Doye, and A. A. Louis, "Sequence-dependent thermodynamics of a coarse-grained DNA model," J. Chem. Phys. **137**, 135101 (2012).
[19]T. Sutthibutpong, C. Matek, C. Benham, G. G. Slade, A. Noy, C. Laughton, J. P. Doye, A. A. Louis, and S. A. Harris, "Long-range correlations in the mechanics of small DNA circles under topological stress revealed by multi-scale simulation," Nucl. Acids Res. **44**, 9121–9130 (2016).
[20]A. Fathizadeh, B. Eslami-Mossallam, and M. R. Ejtehadi, "Definition of the persistence length in the coarse-grained models of DNA elasticity," Phys. Rev. E **86**, 051907 (2012).
[21]K. Huang, *Statistical Mechanics* (J. Wiley, 1987).
[22]T. E. Ouldridge, A. A. Louis, and J. P. Doye, "Structural, mechanical, and thermodynamic properties of a coarse-grained DNA model," J. Chem. Phys. **134**, 085101 (2011).
[23]C. Matek, T. E. Ouldridge, J. P. Doye, and A. A. Louis, "Plectoneme tip bubbles: Coupled denaturation and writhing in supercoiled DNA," Sci. Rep. **5**, 7655 (2015).
[24]F. Lankaš, J. Šponer, J. Langowski, and T. E. Cheatham, "DNA basepair step deformability inferred from molecular dynamics simulations," Biophys. J. **85**, 2872–2883 (2003).
[25]B. Eslami-Mossallam and M. Ejtehadi, "Asymmetric elastic rod model for DNA," Phys. Rev. E **80**, 011919 (2009).
[26]C. Brackley, A. Morozov, and D. Marenduzzo, "Models for twistable elastic polymers in Brownian dynamics, and their implementation for LAMMPS," J. Chem. Phys. **140**, 135103 (2014).
[27]J. Marko, "Stretching must twist DNA," Europhys. Lett. **38**, 183 (1997).
[28]J. Gore, Z. Bryant, M. Nöllmann, M. U. Le, N. R. Cozzarelli, and C. Bustamante, "DNA overwinds when stretched," Nature **442**, 836–839 (2006).
[29]T. Lionnet and F. Lankaš, "Sequence-dependent twist-stretch coupling in DNA," Biophys. J. **92**, L30–L32 (2007).
[30]M. Upmanyu, H. Wang, H. Liang, and R. Mahajan, "Strain-dependent twist–stretch elasticity in chiral filaments," J. R. Soc., Interface **5**, 303–310 (2008).
[31]M. Y. Sheinin and M. D. Wang, "Twist–stretch coupling and phase transition during DNA supercoiling," Phys. Chem. Chem. Phys. **11**, 4800–4803 (2009).
[32]J. Lipfert, G. M. Skinner, J. M. Keegstra *et al.*, "Double-stranded RNA under force and torque: Similarities to and striking differences from double-stranded DNA," Proc. Natl. Acad. Sci. U. S. A. **111**, 15408–15413 (2014).
[33]T. Dršata, N. Špačková, P. Jurečka, M. Zgarbová, J. Šponer, and F. Lankaš, "Mechanical properties of symmetric and asymmetric DNA A-tracts: Implications for looping and nucleosome positioning," Nucl. Acids Res. **42**, 7383–7394 (2014).
[34]T. Lepage, F. Képès, and I. Junier, "Thermodynamics of long supercoiled molecules: Insights from highly efficient Monte Carlo simulations," Biophys. J. **109**, 135–143 (2015).
[35]A. Fathizadeh, H. Schiessel, and M. Ejtehadi, "Molecular dynamics simulation of supercoiled DNA rings," Macromolecules **48**, 164–172 (2015).
[36]N. B. Becker and R. Everaers, "DNA nanomechanics: How proteins deform the double helix," J. Chem. Phys. **130**, 04B602 (2009).
[37]J. F. Marko, "Biophysics of protein-DNA interactions and chromosome organization," Physica A **418**, 126–153 (2015).